



The influence of ice sheets on the climate during the past 38 million years

Lennert B. Stap¹, Roderik S. W. van de Wal¹, Bas de Boer¹, Richard Bintanja², and Lucas J. Lourens³

¹Institute for Marine and Atmospheric research Utrecht (IMAU), Utrecht University, Princetonplein 5, 3584 CC Utrecht, The Netherlands

²Royal Netherlands Meteorological Institute (KNMI), Wilhelminalaan 10, 3732 GK De Bilt, The Netherlands

³Department of Earth Sciences, Faculty of Geosciences, Utrecht University, Heidelberglaan 2, 3584 CS Utrecht, The Netherlands

Correspondence to: Lennert B. Stap (L.B.Stap@uu.nl)

Abstract. Since the inception of the Antarctic ice sheet at the Eocene-Oligocene Transition (~34 Myr ago), land ice has played a crucial role in Earth's climate. Through the ice-albedo and surface-height-temperature feedbacks, land ice variability strengthens atmospheric temperature changes induced by orbital and CO₂ variations. Quantification of these feedbacks on long time scales has hitherto scarcely been undertaken. In this study, we use a zonally averaged energy balance climate model bi-directionally coupled to a one-dimensional ice sheet model. The relative simplicity of these models allows us to perform integrations over the past 38 Myr in a fully transient fashion, using a benthic oxygen isotope record as forcing to inversely simulate CO₂. Output of the model are mutually consistent records of CO₂, temperature, ice volume-equivalent sea level and benthic δ¹⁸O. Firstly, we investigate the relation between global temperature and CO₂, which changes once the model run has experienced high CO₂ concentrations. Secondly, we study the influence of ice sheets on the evolution of global temperature and polar amplification by comparing runs with ice sheet-climate interaction switched on and off. We find that ice volume variability has a strong enhancing effect on atmospheric temperature changes, particularly in the regions where the ice sheets are located. As a result, polar amplification in the Northern Hemisphere decreases towards warmer climates as there is little land ice left to melt. Conversely, decay of the Antarctic ice sheet increases polar amplification in the Southern Hemisphere in the high-CO₂ regime. Our results also show that in cooler climates than the pre-industrial, the ice-albedo feedback predominates the surface-height-temperature feedback, while in warmer climates they are more equal in strength.

1 Introduction

The most abundant information source with the highest resolution on Cenozoic global climate change are stacked benthic oxygen isotope (δ¹⁸O) records (Lisiecki and Raymo, 2005; Zachos et al., 2008; Cramer et al., 2009), which have been well-studied and statistically analysed (e.g. Mudelsee et al., 2014). The benthic δ¹⁸O signal is known to be comprised of two factors (e.g. Chappell and Shackleton, 1986): 1) the deep-sea temperature, and 2) the volume of land ice on Earth. An additional independent record of either one is therefore required to separate the signal into its individual constituents. Deep-sea temperature records can be reconstructed based on the Mg/Ca proxy (Lear et al., 2000; Sosdian and Rosenthal, 2009; Elderfield et al.,



2012), but a global average deep-sea temperature is hard to obtain. Sea level records are also available, but are subject to the same problem of inferring a global mean (Miller et al., 2005; Kominz et al., 2008; Rohling et al., 2014). Studies using sea level records face the additional challenge of converting local sea level to ice volume, which is not straightforward mainly because of dynamic topography (Mitrovica and Milne, 2003; Kendall et al., 2005). Alternatively, calculation of benthic $\delta^{18}\text{O}$ can be incorporated in coupled ice sheet-climate models, by using parameterisations of the contribution of deep-sea temperature (Duplessy et al., 2002), and the isotopic content of ice sheets (Cuffey, 2000). Hitherto, studies using this approach have mostly focused on relatively short time intervals surrounding important climatic events, such as the Eocene-Oligocene Transition (33.9 Myr ago; Tigchelaar et al. (2011); Ladant et al. (2014); Wilson et al. (2013)), the Mid-Miocene Climatic Optimum (13.9 Myr ago; Langebroek et al. (2010); Gasson et al. (2016)), and the Pliocene-Pleistocene Transition (2.6 Myr ago, Willeit et al. (2015)), using models of varying complexity. Computer power remains a limiting factor for these coupled ice sheet-climate studies. Nevertheless, a study using a model of reduced complexity simulated the past 3 million years (Berger et al., 1999). However, they did not include the Southern Hemisphere and the Antarctic ice sheet in their model. Here, we will use a coupling between an energy balance global climate model and a one-dimensional ice sheet model of all major ice sheets, to perform transient simulations over the past 38 Myr.

Our model approach builds on the inverse routine to derive atmospheric temperature from benthic $\delta^{18}\text{O}$, that was introduced by Oerlemans (2004). This methodology was consequently developed further to force stand-alone three-dimensional ice sheet models over the past 1 Myr (Bintanja et al., 2005; De Boer et al., 2013), the past 3 Myr (Bintanja and Van de Wal, 2008), and the past 5 Myr (De Boer et al., 2014). With this inverse routine, the past 40 Myr were simulated (De Boer et al., 2010) and further analysed (De Boer et al., 2012), using a one-dimensional ice sheet model that calculates all land ice on Earth. In Stap et al. (2014), this ice sheet model was coupled to a zonally averaged energy balance climate model (Bintanja, 1997), and run over the past 800 kyr forced by the EPICA Dome C ice-core CO_2 record (EPICA community members, 2004). Inclusion of a climate model added CO_2 to global temperature and sea level as an integrated component of the simulated system. In addition, it rendered the possibility of investigating ice sheet-climate interactions, specifically the ice-albedo and surface-height-temperature feedbacks. Furthermore, instead of annual mean and globally uniform temperature perturbations to present-day climate, seasonal meridional temperature distributions were used to force the different ice sheets. In a subsequent study, the inverse routine was transformed to yield CO_2 concentrations using the benthic $\delta^{18}\text{O}$ as input, making CO_2 a prognostic variable (Stap et al., 2016a). The resulting values were used to force the coupled model over the past 5 Myr. In Stap et al. (2016b), the model was run over the period 38 to 10 Myr ago, and the influence of Antarctic topographic changes on the simulated CO_2 was investigated.

Here, we will first explore a hysteresis that occurs in our coupled model, which necessitates us to reconfigure our setup. Using a new reference simulation, we will attempt to quantify the influence of ice sheets on climate change during the past 38 million years, specifically on global temperature perturbations and polar amplification. To this end, we compare runs of the climate model where ice sheet-climate interaction is switched off to the new reference run. We find that ice sheets modify the Earth System Sensitivity more strongly in cooler climates. Furthermore, they have a large regional impact, which causes CO_2 -induced climate change to be heavily dependent on latitude. Moreover, polar amplification is determined by the background climate state.



2 Methodology

We use the same simplified coupled ice sheet-climate model setup as Stap et al. (2016b) (Fig. 1). The climate component is a zonally averaged energy balance climate model (based on North, 1975; Bintanja, 1997) with 5° latitudinal resolution, including a simple ocean model mimicking meridional seawater circulation with varying strength based on the density difference between the polar and equatorial waters. The climate model provides the temperature input (T) to the mass balance module of a one-dimensional ice sheet model that uses the Shallow Ice Approximation. The ablation (M) in the mass balance parameterisation is calculated by an insolation-temperature melt equation:

$$M = [10T + 0.513(1 - \alpha)Q + C_{abl}]/100. \quad (1)$$

Here, α is surface albedo, and Q local radiation obtained from Laskar et al. (2004). Ice-sheet dependent tuning factors C_{abl} determine the threshold for which ablation starts (listed in Stap et al., 2014). The ice sheet model (De Boer et al., 2010) calculates the surface height change and ice sheet extent of five ice sheets on Earth: Greenland, North America, Eurasia, East Antarctica and West Antarctica. This information is used to update the land ice fraction and surface height profile in the climate model for the next time step. Exchange of variables takes place every 500 model years. The coupled model is forced with insolation data (Laskar et al., 2004) and an inverse routine, which yields CO₂ concentrations from the difference between the modeled benthic $\delta^{18}\text{O}$ value and an observed value an output-timestep later (Stap et al., 2016a). The radiative forcing anomaly with respect to present day is multiplied by a factor 1.3 to account for non-CO₂ greenhouse gases. The result of the model consists of mutually consistent records of benthic $\delta^{18}\text{O}$, atmospheric CO₂, temperature, and ice-volume equivalent sea level.

First, we extend the run over the period 38 to 10 Myr ago forced with the stacked benthic $\delta^{18}\text{O}$ of Zachos et al. (2008) described in Stap et al. (2016b), to include the past 10 Myr (this run is called '38 Myr'). We compare the results of the past 5 Myr to the reference run of Stap et al. (2016a), that simulated the past 5 Myr using the record of Lisiecki and Raymo (2005) as forcing (this run is called '5 Myr'). The 38 Myr run shows CO₂ values that are much lower over the past 5 Myr than the results of the old reference run, and therefore also far below the EPICA Dome C record (EPICA community members, 2004). To regain agreement with the EPICA Dome C record, we define a new reference run in this study (new REF). In this new reference run we increase the cloud optical thickness parameter τ_{cl} from 3.11 to 3.41. We opt to alter this parameter because it was already used as a tuning parameter in the original climate model (Bintanja, 1997), and in the ice sheet-climate model coupling (Stap et al., 2014). Increasing τ_{cl} will lower the temperatures calculated by the climate model, such that for the same benthic $\delta^{18}\text{O}$ higher simulated CO₂ levels are obtained, in better agreement with the EPICA Dome C record. However, this will also raise the threshold CO₂ level for the inception of the East Antarctic ice sheet (EAIS). By increasing the ablation threshold parameter C_{abl} in the insolation-temperature-melt calculation (Eq. (1)) of the EAIS (from -30 to -10), this ice sheet glaciates at lower temperatures and therefore at lower CO₂ concentrations. This compensates the unintended CO₂ threshold increase. In this run, the Zachos et al. (2008) record is once more used to force the model over the past 38 Myr after a 2 Myr spin-up, similarly as in Stap et al. (2016b). Furthermore, to study the effect of ice sheet-climate interactions, we perform three model tests over the past 38 Myr, where we use the same CO₂ input as the new reference run, but keep the ice sheet extent and



surface height constant at present-day (PD ice/ice uncoupled) or Last Glacial Maximum (LGM ice) level, or remove all ice in the climate model completely (no ice). In two last tests, we keep the surface height constant at present-day (PD) level, but still vary ice sheet extent (height uncoupled) or oppositely keep the ice sheet extent at PD level and only vary the surface height (albedo uncoupled). This allows us to distinguish the effects of the surface-height-temperature feedback and the ice-albedo feedback. We show 40-kyr running averages of all variables, because shorter scale variability is too strong in our model during the period 38 to 10 Myr ago (see Stap et al., 2016b).

To further explore the difference we find between the results of the 5 Myr and the 38 Myr run, we additionally conduct four pairs of experiments with the model in forward mode. In forward mode, we do not use the inverse routine, but force the model by a-priori designed CO₂ scenarios. We run the model fully coupled, or alternatively by keeping ice sheets (PD ice), or ocean overturning strength (PD OT), or both (PD ice + OT) constant at their present-day levels. Starting from a CO₂ concentration of 450 ppm, we force the model by changing the CO₂ input in steps of 50 ppm every 50 kyr. In one set of experiments (named 'up'), the CO₂ is first raised from 450 ppm to 1200 ppm, then lowered to 150 ppm, and increased again to 600 ppm. In the other set (named 'down'), the CO₂ is initially dropped from 450 to 150 ppm, then raised to 1200 ppm, and ultimately decreased again to 300 ppm. Insolation is kept at PD level in all these equilibrium experiments, and the parameters of the coupled model are set to their old reference values ($C_{abl} = -30$ for the EAIS, and $\tau_{cl} = 3.11$) (Stap et al., 2014, 2016b).

3 Results: hysteresis and new reference

When we compare the final 5 Myr of our 38-Myr simulation to our 5-Myr simulation, we notice that the 38-Myr simulation shows much lower CO₂ concentrations (Fig. 2b, green and blue lines). These contradicting results cannot be explained by the use of different forcing records - Zachos et al. (2008) for 38 Myr as opposed to Lisiecki and Raymo (2005) for 5 Myr - as these show similar values during this time (0.02 ‰ average difference, not shown). Instead, this incongruence is caused by model hysteresis, to wit a dependency of the simulated global temperature on the evolution of CO₂ during the run as well as the prevailing CO₂ level. This becomes apparent when we study the relation between CO₂ and global temperature in the forward runs with stepwise changing CO₂ described in Sect. 2, performed with the fully coupled model (Fig. 3a). Starting at 450 ppm CO₂, the 'up' and 'down' runs show the same initial global temperature. However, in the 'down' run, where the CO₂ progresses stepwise downward first and then upward, the global temperatures at low (< 450 ppm) CO₂ values are approximately a degree lower than those in the 'up' run, where CO₂ is first raised and then lowered. When the 'down' run is integrated over another CO₂ cycle, it shows the same global temperatures as the up run (not shown). This means that once the coupled model has experienced high CO₂ values during its run, as is the case in the 38-Myr run but not in the 5-Myr run, the climates at lower CO₂ are warmer. This has important consequences for the simulated CO₂ concentrations as they have to decline further to obtain similar temperature values, which is what happens in the transient 38-Myr simulation forced by the inverse routine. This behavior is a form of hysteresis as results depend on previous conditions of the model. The question now arises what the cause of this hysteresis is. The global temperature difference between the 'up' and 'down' run is 0.94 K at 150 ppm CO₂. When the ice sheet model is uncoupled, and the climate model is directly forced by PD ice sheets, this reduces



to 0.69 K (Fig. 3b, blue and cyan lines). Keeping the ocean overturning strength fixed at PD also leads to a small reduction; the difference becomes 0.73 K (Fig. 3b, dark green and light green lines). The combined effect of uncoupled ice and ocean overturning strength is still not sufficient to eliminate the hysteresis (Fig. 3b, red and orange lines). Even when in addition sea ice and snow cover are kept constant, a small hysteresis is present (not shown). This means that the hysteresis is inherent to the core of the climate model: the parameterisation of vertical and horizontal energy transfer in the ocean and atmosphere. The factors mentioned above act to enhance this hysteresis.

Over the past 800 kyr, the 5-Myr run was calibrated to the EPICA Dome C ice core proxy- CO_2 record (EPICA community members, 2004) and shows negligible bias (-3.9 ppm), whereas with the same parameter setting the 38-Myr run shows much lower values than this proxy record with a -47.7 ppm bias (Fig. 2a, mind that here we show 1-kyr values instead of 40-kyr averages). The simulated CO_2 over the past 5 Myr in the 38-Myr run is also much lower than the hybrid proxy data-model reconstruction by Van de Wal et al. (2011) (Fig. 2b, black line). Therefore, we deduce that the CO_2 record of the 38-Myr run is probably not realistic over this period. In order to obtain a more realistic 38-Myr simulation in closer agreement with the EPICA record, we modify the relation between CO_2 and atmospheric temperature. We accomplish this by increasing the cloud optical thickness parameter in the climate model, with lower temperatures at the same CO_2 levels as result (see Sect. 2). As a consequence, the same benthic $\delta^{18}\text{O}$ values can be achieved at higher CO_2 . The threshold CO_2 value for glaciation of the East Antarctic ice sheet is maintained at a similar level as before by decreasing ablation on this ice sheet.

Now, forcing the model with Zachos et al. (2008), we obtain a new reference simulation over the past 38 Myr (Fig. 2, red lines). The simulated CO_2 levels right before the Eocene-Oligocene Transition (EOT; ~ 33.9 Myr ago) and at the Middle-Miocene Climatic Optimum (MMCO; 17 to 15 Myr ago) are similarly high around 650 to 750 ppm, likewise as in the earlier 38-Myr simulation (Fig. 2c). In the time between these events, CO_2 in the new reference run is modestly higher, up to 100 ppm. This is because the deep-sea temperatures are lower at the same CO_2 , and therefore contribute less to the $\delta^{18}\text{O}$ anomaly with respect to present day. Compensating for the lower deep-sea temperatures, higher CO_2 increases the $\delta^{18}\text{O}$ anomaly, by increasing both deep-sea temperature and the contribution of ice volume, hence raising sea levels (not shown). After the MMCO, when the EAIS has stabilised to near-PD size, the new reference simulation shows higher CO_2 values. Over the past 25 million years, the new reference simulation (Fig. 2a, red line) agrees much better with the 5-Myr run (Fig. 2a, green line) and with the EPICA proxy- CO_2 record (Fig. 2a, cyan line); the bias with respect to this proxy-record is reduced to 13.6 ppm. Even after re-calibration, the simulated new reference CO_2 remains lower than in the 5-Myr run during the Pliocene and early Pleistocene (Fig. 2b, green line), as a consequence of the hysteresis. Although it is more variable than the reconstruction based on a constant Earth System Sensitivity (ESS) by Van de Wal et al. (2011) (Fig. 2b, black line), the long-term means are now 30 similar.

4 Results: ice sheet-climate interaction

In this section, we investigate the influence of ice sheet-climate interaction on polar amplification, and on the Earth System Sensitivity (ESS). The ESS is defined as the global temperature response to a radiative forcing caused by changing CO_2 , tak-



ing into account all climate feedbacks (PALAEOSENS Project Members, 2012). This radiative forcing by CO_2 is proportional to the logarithmic change of CO_2 (Myhre et al., 1998). In Fig. 4 (red dots), we therefore show the relation between global temperature anomalies from pre-industrial (PI) and the logarithm of CO_2 divided by a reference PI value of 280 ppm in our new reference run. Evidently, this relation is not constant, as in warm climates the global temperature increase for a given CO_2 increase is less strong. The slope of a least squares linear regression shows a value of 10.6 K for $\ln(\text{CO}_2/\text{CO}_{2,\text{ref}})$ values below 0 ($\text{CO}_2 < 280$ ppm: coldest climates), and 3.7 K for values above 0.69 ($\text{CO}_2 > 560$ ppm: warmest climates), a reduction of 65 %. In the ice uncoupled run, the slope reduces by only 46 % from 5.6 K to 3.0 K going from the coldest to the warmest $\ln(\text{CO}_2/\text{CO}_{2,\text{ref}})$ regime (Fig. 4, blue dots). In this case, the standard error of an linear regression through all data points is reduced by 58 % with respect to the fully coupled run, from 0.0050 K to 0.0021 K. The fact that the relation between $\ln(\text{CO}_2/\text{CO}_{2,\text{ref}})$ and global temperature is better approximated by a linear fit when land ice is uncoupled means the log(CO_2)-T relation is more linear. The coldest anomaly is amplified by 79 % (factor 1.79) if land ice changes are incorporated, by 50 % if only albedo is coupled (Fig. 4, black dots), and by 4 % if only surface height is coupled (Fig. 4, orange dots). The warmest anomaly is only increased by 21 % (factor 1.21) when ice is coupled, by 9 % when only albedo is coupled, and by 3 % when only surface height is coupled. This means the surface-height-temperature feedback becomes relatively more important in warmer climates. Since decreased ESS at higher CO_2 is still present in the run where ice volume is kept at PD level (Fig. 4, blue dots), reduced ice volume variability is not its only determining factor.

The influence of ice sheets on the climate is strongest in the region where they are situated, leading to increased polar amplification. This is demonstrated by the relation between global temperature and Northern Hemispheric (40 to 80° N, Fig. 5a), or Antarctic temperature (60 to 90° S, Fig. 5b). In the Northern Hemisphere, the minimum local temperature with respect to PI is -2.0 K in the uncoupled case, and -9.5 K in the run with fully coupled land ice. When only the albedo or surface height changes are coupled, the Northern Hemispheric temperature anomaly reaches -6.4 K and -2.8 K low points respectively. Conversely, the amount of land ice lost in warmer climates is relatively small, as only the Greenland ice sheet (~ 7 m.s.l.e.) is left to melt. Consequently, the Northern Hemispheric temperature is then not affected much by not including land ice changes. The remaining polar amplification in the Northern Hemisphere is hence mostly caused by other factors, such as sea ice and snow cover variability. In the Southern Hemisphere, the lowest temperature is similar for the coupled and uncoupled simulations, although it is achieved at a higher global temperature in the uncoupled case. These Southern Hemispheric temperatures are similarly low because the Antarctic ice sheet grows relatively little in size towards colder-than-PI conditions (see also Stap et al., 2014). When Antarctica is allowed to melt in warm climates, however, the local temperature increase becomes much stronger: 11.6 instead of 5.9 K with respect to PI. In these conditions, we find that coupling albedo changes leads to a maximum Antarctic temperature anomaly of only 7.0 K (Fig. 5b, black dots). When only surface height changes are coupled, this anomaly reaches 7.4 K (Fig. 5b, orange dots). This result implies that albedo changes are relatively less important in Antarctica than in the high latitudes of the Northern Hemisphere. The reason is that the Antarctic continent remains snow covered throughout most of the year when the land ice retreats, which reduces the albedo change (see also Stap et al., 2016a). Since temperature changes are strongest in the Southern Hemisphere in warmer-than-PI climates, this explains the increased relative importance of the surface-height-temperature feedback on ESS in these climates.



Finally, we compare the relation between global temperature and logarithmic CO_2 in three model runs with uncoupled ice (Fig. 6). In one run the ice sheets are kept at PD condition as before (now called PD ice, blue dots), in another one we use the LGM condition (LGM ice, black dots), and in the last one all ice is removed (no ice, red dots). Naturally, the more ice is present on Earth, the colder the climate becomes, so the LGM ice run is colder than the PD ice run, which in turn is colder than the no ice run. The difference between the PD ice and the no ice run is fairly uniform over the whole CO_2 range. The difference between the LGM ice and the no ice run, however, is larger in cold climates than in warm climates as it shrinks from ~ 2.8 to ~ 1.6 K. This is explained by the extra land ice in the LGM ice run cooling the climate and increasing the area on Earth covered by snow and sea ice. As a result of this area increase, the land surface has a higher albedo, which cools the climate further. In cold climates this effect is stronger because the snow- and sea ice-covered area grows more towards the equator, where there is more incoming solar radiation. Consequently, the albedo increase is more effective as it leads to absorption of more energy, and thus to a stronger temperature decrease.

5 Discussion and conclusions

We have presented mutually consistent transient simulations of CO_2 , temperature, ice volume and benthic $\delta^{18}\text{O}$ over the past 38 million years. They were obtained using a coupling between a zonally averaged energy balance climate model and a one-dimensional ice sheet model. A similar coupled ice sheet-climate model of reduced complexity was introduced by Gallée et al. (1992): the LLN-2D model. However, in contrast to the LLN-2D model we include the Southern Hemisphere and the Antarctic ice sheet. Furthermore, we use an inverse routine that yields atmospheric CO_2 from an observed benthic $\delta^{18}\text{O}$ record (Zachos et al., 2008). This allows us to simulate periods further back in time, for which CO_2 data are highly uncertain (Beerling and Royer, 2011), and when the Antarctic ice sheet was very dynamic. This constitutes a wider simulated range of climates. For a comparison between the results of our model and the LLN-2D model, the reader is referred to Stap et al. (2014). Our coupled model also represents an improvement upon the model setup of De Boer et al. (2010), who used the same ice-sheet model in stand-alone form to simulate the past 40 Myr (De Boer et al., 2010, 2012). The inclusion of a climate model enables us to simulate, and force the different ice sheets with, seasonal meridional temperature distributions instead of globally uniform perturbations to present-day climate with a fixed seasonal cycle. Nonetheless, we recognise that our coupled ice sheet-model is relatively simple. However, more sophisticated models, such as GCMs coupled to three-dimensional thermodynamic ice models, are as of yet not suitable to perform multi-million year integrations, because of limited computer power. Our results should therefore be seen as a first step in the direction of simulating these time spans with coupled ice sheet-climate models, thereby identifying interesting phenomena and potential obstacles. When results of these more sophisticated models are achieved, they can be compared to ours to see which features appear in the full hierarchy of models and which are specific to more comprehensive models including more physics.

In our model, the results for CO_2 concentrations lower than roughly 450 ppm depend on the transient evolution of CO_2 . When during the run the model has previously experienced high CO_2 values, temperatures are higher than when this is not the case. This hysteresis is persistent even in runs without any change in albedo due to snow-, sea ice- or permanent land ice-cover



and without changes in ocean overturning strength. However, these factors do enhance it. The hysteresis leads to a mismatch in runs over the past 38 Myr between the CO₂ concentrations of the past 800 kyr and the EPICA Dome C proxy-record. Since this proxy record served as a main target for our model performance (see Stap et al., 2016a), we have re-calibrated the model configuration. We have achieved more satisfactory results by increasing the cloud optical thickness parameter, which decreases temperatures in the climate model. Therefore, simulated CO₂ concentrations are higher, in order to obtain the same benthic δ¹⁸O values. However, even after this re-calibration, simulated CO₂ values are still lower than in the 5-Myr run of Stap et al. (2016a). It remains debatable which simulation is the most veracious over the past 5 Myr. On the one hand, the long simulation carries a longer memory, which would be closer to the state of the actual climate system. On the other hand, it is uncertain how accurately our climate model simulates very warm climates; the climate model is designed and tested for PD and LGM climates (Bintanja and Oerlemans, 1996). This argument favours the shorter 5-Myr run as the more trustworthy result. Regardless, it remains unknown whether the hysteresis is an artefact of our model, or is also exhibited by other models. We therefore suggest that in the future, climate models should be tested for this behaviour by confronting them with high CO₂ values before simulating cooler climates.

The relation between temperature and ice volume in our model can roughly be divided into three regimes (see also De Boer et al. (2010) and Van de Wal et al. (2011)): 1) at low CO₂ values, strong ice volume variability due to dynamic Northern Hemispheric ice sheets, 2) at intermediate CO₂ values, weaker variability, 3) at high CO₂ values, strong variability due to a dynamic Antarctic ice sheet. This constitutes a sigmoidal temperature-sea level relation, similar to the data-analysis results of Gasson et al. (2012). A sigmoidal shape is also apparent in the modeled relation between logarithmic CO₂ and sea level, coherent with the results from Foster and Rohling (2013). The threshold CO₂ value for glaciation of the Southern Hemisphere is distinctly higher than for the Northern Hemisphere in our model, which was also found by DeConto et al. (2008). In our model, this is a consequence of lower forcing temperatures, as the Antarctic ice sheet initiates at higher latitudes.

When ice sheets are kept at PD level, the relation between logarithmic CO₂ and global temperature shows a declining slope. This may be compared to the hybrid data-model results for climate sensitivity of Köhler et al. (2015), as well as to the modeled climate sensitivity of Friedrich (2015). Köhler et al. (2015) investigated the relation between the radiative forcing of proxy-data CO₂ (EPICA community members, 2004; Hönlisch et al., 2009) - which is linearly related to logarithmic CO₂ (Myhre et al., 1998) - and modeled global temperature (De Boer et al., 2014, scaled). Friedrich (2015) forced the intermediate complexity climate model LOVECLIM over the past 800 kyr using the EPICA Dome C ice-core record (EPICA community members, 2004) and an Northern Hemispheric ice sheet reconstruction (Ganopolski and Calov, 2011). The resulting climate sensitivity of these studies is opposite to ours, as they show increased climate sensitivity at higher CO₂ concentrations. These studies, however, consider a smaller range of CO₂. Furthermore, their approach is different, as they do take into account ice volume variations, but compensate for their effect by adding their radiative forcing to the forcing induced by CO₂ variations (see PALAEOSENS Project Members, 2012). Implicitly assumed in their approach is that these radiative forcings have the same effect on temperature, which may not generally be the case (Yoshimori et al., 2011). Our findings are in agreement with Ritz et al. (2011), who used a two-dimensional energy balance climate model that showed an increase of climate sensitivity from 3.0 K per CO₂ doubling at PI conditions to 4.3 K at LGM conditions.



Ice volume changes enhance the modeled effect of CO₂ on temperature, via the ice-albedo and the surface-height-temperature feedbacks. As the growth and decay of the Antarctic ice sheet is spread over a larger range of logarithmic CO₂, this effect is stronger on the low CO₂ branch than on the high CO₂ branch. This leads to an increased curve in the ln(CO₂)-temperature relation when land ice is allowed to vary. We do not find Earth System Sensitivity (ESS) to be constant, opposite to the implicit
5 assumption in Van de Wal et al. (2011). In fact, in our model ESS is stronger at lower CO₂, similar to the findings of Hansen et al. (2013), who performed CO₂ doubling experiments using the simplified atmosphere-ocean model of Russell et al. (1995). However, their ESS is consistently higher than what our model calculates. They eventually also find increased sensitivity again at high CO₂ (2480 to 9920 ppm), which is outside the range we simulate during our time span.

Our results further clearly show a non-linear relation between temperatures on both hemispheres, caused by asymmetric ice
10 sheet-climate interaction. In cooler climates, the Northern Hemispheric ice sheets change in size, causing large fluctuations in the temperature on this hemisphere. The ice-albedo feedback is much stronger than the surface-height-temperature feedback in these conditions (see also Stap et al., 2014). This is reflected in the Northern Hemispheric (40 to 80° N), Antarctic (60 to 90° S), and global temperature profiles. Oppositely, in warmer climates the Antarctic ice sheet is more dynamic, so that temperature changes more strongly on the Southern Hemisphere. Now, the surface-height-temperature feedback becomes relatively more
15 important. When the ice sheets are kept constant, the temperature perturbations are more uniformly distributed over the globe. The different response of the northern and southern high latitudes to CO₂ changes challenges the approach of De Boer et al. (2010) and De Boer et al. (2012), who reconstructed a single high-latitude temperature anomaly. Furthermore, their record cannot readily be translated to global conditions by a constant factor (as is done in e.g. Martínez-Botí et al., 2015), because the conversion depends on the prevailing climate state. This also holds for the interpretation of proxy data from high northern and
20 southern latitudes, both marine and ice cores.

Future work on polar amplification and ESS on long timescales may involve using more sophisticated models. When results of these models become available, a comparison to this work can be made, to see what the added complexity invokes in the simulated system. Alternatively, the simplified model used here can be extended with more aspects of the climate system, moving towards a full Earth System Model. Important aspects hitherto neglected in our model are the effects of dynamic vegetation
25 (e.g. Knorr et al., 2011; Liakka et al., 2014), dynamic topography (Mitrovica and Milne, 2003; Kendall et al., 2005), and land surface changes (e.g. tectonics, sedimentation) (Stap et al., 2016b; Wilson et al., 2012; Gasson et al., 2015). Ultimately, this model could also be coupled to a carbon cycle model, e.g. BICYCLE (Köhler and Fischer, 2004), in order to simulate climate using only insolation data as input.

Author contributions. L.B.S., R.S.W.v.d.W. and B.d.B. designed the research. B.d.B., R.B., and L.B.S. developed the model. L.B.S. conducted the model runs and analysis, to which R.S.W.v.d.W. and B.d.B contributed. L.B.S. drafted the manuscript, with contributions from all
30 co-authors.

Competing interests. The authors declare that they have no conflict of interest.

Clim. Past Discuss., doi:10.5194/cp-2016-109, 2016

Manuscript under review for journal Clim. Past

Published: 8 November 2016

© Author(s) 2016. CC-BY 3.0 License.



Acknowledgements. Financial support for L.B. Stap was provided by the Netherlands Organisation of Scientific Research (NWO), grant NWO-ALW. Bas de Boer is funded by NWO Earth and Life Sciences (ALW), project 863.15.019. This paper contributes to the gravity program "Reading the past to project the future", funded by the Netherlands Organisation for Scientific Research (NWO).



References

- Berling, D. J. and Royer, D. L.: Convergent Cenozoic CO₂ history, *Nature Geoscience*, 4, 418–420, 2011.
- Berger, A., Li, X. S., and Loutre, M.-F.: Modelling Northern Hemisphere ice volume over the last 3Ma, *Quaternary Science Reviews*, 18, 1–11, 1999.
- 5 Bintanja, R.: Sensitivity experiments performed with an energy balance atmosphere model coupled to an advection-diffusion ocean model, *Theoretical and Applied climatology*, 56, 1–24, 1997.
- Bintanja, R. and Oerlemans, J.: The effect of reduced ocean overturning on the climate of the Last Glacial Maximum, *Climate Dynamics*, 12, 523–533, 1996.
- Bintanja, R. and Van de Wal, R. S. W.: North American ice-sheet dynamics and the onset of 100,000-year glacial cycles, *Nature*, 454, 869–872, 2008.
- 10 Bintanja, R., van de Wal, R. S. W., and Oerlemans, J.: Modelled atmospheric temperatures and global sea levels over the past million years, *Nature*, 437, 125–128, 2005.
- Chappell, J. and Shackleton, N. J.: Oxygen isotopes and sea level, *Nature*, 324, 137–140, 1986.
- Cramer, B. S., Toggweiler, J. R., Wright, J. D., Katz, M. E., and Miller, K. G.: Ocean overturning since the Late Cretaceous: Inferences from a new benthic foraminiferal isotope compilation, *Paleoceanography*, 24, 2009.
- 15 Cuffey, K. M.: Methodology for use of isotopic climate forcings in ice sheet models, *Geophysical Research Letters*, 27, 3065–3068, 2000.
- De Boer, B., Van de Wal, R. S. W., Bintanja, R., Lourens, L. J., and Tuenter, E.: Cenozoic global ice-volume and temperature simulations with 1-D ice-sheet models forced by benthic $\delta^{18}\text{O}$ records, *Annals of Glaciology*, 51, 23–33, 2010.
- De Boer, B., Van de Wal, R. S. W., Lourens, L. J., and Bintanja, R.: Transient nature of the Earth's climate and the implications for the interpretation of benthic $\delta^{18}\text{O}$ records, *Palaeogeography, Palaeoclimatology, Palaeoecology*, 335, 4–11, 2012.
- 20 De Boer, B., Van de Wal, R. S. W., Lourens, L. J., Bintanja, R., and Reerink, T. J.: A continuous simulation of global ice volume over the past 1 million years with 3-D ice-sheet models, *Climate Dynamics*, 41, 1365–1384, 2013.
- De Boer, B., Lourens, L. J., and Van de Wal, R. S. W.: Persistent 400,000-year variability of Antarctic ice volume and the carbon cycle is revealed throughout the Plio-Pleistocene, *Nature communications*, 5, 2014.
- 25 DeConto, R. M., Pollard, D., Wilson, P. A., Pälike, H., Lear, C. H., and Pagani, M.: Thresholds for Cenozoic bipolar glaciation, *Nature*, 455, 652–656, 2008.
- Duplessy, J.-C., Labeyrie, L., and Waelbroeck, C.: Constraints on the ocean oxygen isotopic enrichment between the Last Glacial Maximum and the Holocene: Paleoceanographic implications, *Quaternary Science Reviews*, 21, 315–330, 2002.
- Elderfield, H., Ferretti, P., Greaves, M., Crowhurst, S., McCave, I. N., Hodell, D., and Piotrowski, A. M.: Evolution of ocean temperature and ice volume through the Mid-Pleistocene climate transition, *Science*, 337, 704–709, 2012.
- 30 EPICA community members: Eight glacial cycles from an Antarctic ice core, *Nature*, 429, 623–628, 2004.
- Foster, G. L. and Rohling, E. J.: Relationship between sea level and climate forcing by CO₂ on geological timescales, *Proceedings of the National Academy of Sciences*, 110, 1209–1214, 2013.
- Friedrich, T.: Global climate sensitivity derived from ~ 784,000 years of SST data, in: 2015 AGU Fall Meeting, Agu, 2015.
- 35 Gallée, H., Van Ypersele, J. P., Fichefet, T., Marsiat, I., Tricot, C. H., and Berger, A.: Simulation of the last glacial cycle by a coupled, sectorially averaged climate-ice sheet model: 2. Response to insolation and CO₂ variations, *Journal of Geophysical Research: Atmospheres* (1984–2012), 97, 15 713–15 740, 1992.



- Ganopolski, A. and Calov, R.: The role of orbital forcing, carbon dioxide and regolith in 100 kyr glacial cycles, *Climate of the Past*, 7, 1415–1425, 2011.
- Gasson, E., Siddall, M., Lunt, D. J., Rackham, O. J. L., Lear, C. H., and Pollard, D.: Exploring uncertainties in the relationship between temperature, ice volume, and sea level over the past 50 million years, *Reviews of Geophysics*, 50, 2012.
- 5 Gasson, E., DeConto, R. M., and Pollard, D.: Antarctic bedrock topography uncertainty and ice sheet stability, *Geophysical Research Letters*, 42, 5372–5377, 2015.
- Gasson, E., DeConto, R. M., Pollard, D., and Levy, R. H.: Dynamic Antarctic ice sheet during the early to mid-Miocene, *Proceedings of the National Academy of Sciences*, 113, 3459–3464, 2016.
- Hansen, J., Sato, M., Russell, G., and Kharecha, P.: Climate sensitivity, sea level and atmospheric carbon dioxide, *Philosophical Transactions of the Royal Society of London A: Mathematical, Physical and Engineering Sciences*, 371, 20120294, 2013.
- 10 Hönlisch, B., Hemming, N. G., Archer, D., Siddall, M., and McManus, J. F.: Atmospheric carbon dioxide concentration across the mid-Pleistocene transition, *Science*, 324, 1551–1554, 2009.
- Kendall, R. A., Mitrovica, J. X., and Milne, G. A.: On post-glacial sea level–II. Numerical formulation and comparative results on spherically symmetric models, *Geophysical Journal International*, 161, 679–706, 2005.
- 15 Knorr, G., Butzin, M., Micheels, A., and Lohmann, G.: A warm Miocene climate at low atmospheric CO₂ levels, *Geophysical Research Letters*, 38, 2011.
- Köhler, P. and Fischer, H.: Simulating changes in the terrestrial biosphere during the last glacial/interglacial transition, *Global and Planetary Change*, 43, 33–55, 2004.
- Köhler, P., de Boer, B., von der Heydt, A. S., Stap, L. B., and van de Wal, R. S. W.: On the state dependency of the equilibrium climate sensitivity during the last 5 million years, *Climate of the Past*, 11, 1801–1823, doi:10.5194/cp-11-1801-2015, 2015.
- 20 Kominz, M. A., Browning, J. V., Miller, K. G., Sugarman, P. J., Mizintseva, S., and Scotese, C. R.: Late Cretaceous to Miocene sea-level estimates from the New Jersey and Delaware coastal plain coreholes: An error analysis, *Basin Research*, 20, 211–226, 2008.
- Ladant, J.-B., Donnadieu, Y., Lefebvre, V., and Dumas, C.: The respective role of atmospheric carbon dioxide and orbital parameters on ice sheet evolution at the Eocene-Oligocene transition, *Paleoceanography*, 29, 810–823, doi:10.1002/2013PA002593, 2014.
- 25 Langebroek, P. M., Paul, A., and Schulz, M.: Simulating the sea level imprint on marine oxygen isotope records during the middle Miocene using an ice sheet-climate model, *Paleoceanography*, 25, 2010.
- Laskar, J., Robutel, P., Joutel, F., Gastineau, M., Correia, A. C. M., Levrard, B., et al.: A long-term numerical solution for the insolation quantities of the Earth, *Astronomy & Astrophysics*, 428, 261–285, 2004.
- Lear, C. H., Elderfield, H., and Wilson, P. A.: Cenozoic deep-sea temperatures and global ice volumes from Mg/Ca in benthic foraminiferal calcite, *Science*, 287, 269–272, 2000.
- 30 Liakka, J., Colleoni, F., Ahrens, B., and Hickler, T.: The impact of climate-vegetation interactions on the onset of the Antarctic ice sheet, *Geophysical Research Letters*, 41, 1269–1276, 2014.
- Lisiecki, L. E. and Raymo, M. E.: A Pliocene-Pleistocene stack of 57 globally distributed benthic $\delta^{18}\text{O}$ records, *Paleoceanography*, 20, 2005.
- Martínez-Botí, M., Foster, G., Chalk, T., Rohling, E., Sexton, P., Lunt, D., Pancost, R., Badger, M., and Schmidt, D.: Plio-Pleistocene climate sensitivity evaluated using high-resolution CO₂ records, *Nature*, 518, 49–54, 2015.
- 35 Miller, K. G., Kominz, M. A., Browning, J. V., Wright, J. D., Mountain, G. S., Katz, M. E., Sugarman, P. J., Cramer, B. S., Christie-Blick, N., and Pekar, S. F.: The Phanerozoic record of global sea-level change, *Science*, 310, 1293–1298, 2005.
- Mitrovica, J. X. and Milne, G. A.: On post-glacial sea level: I. General theory, *Geophysical Journal International*, 154, 253–267, 2003.



- Mudelsee, M., Bickert, T., Lear, C. H., and Lohmann, G.: Cenozoic climate changes: A review based on time series analysis of marine benthic $\delta^{18}\text{O}$ records, *Reviews of Geophysics*, 52, 333–374, 2014.
- Myhre, G., Highwood, E. J., Shine, K. P., and Stordal, F.: New estimates of radiative forcing due to well mixed greenhouse gases, *Geophysical Research Letters*, 25, 2715–2718, 1998.
- 5 North, G. R.: Theory of energy-balance climate models, *Journal of the Atmospheric Sciences*, 32, 2033–2043, 1975.
- Oerlemans, J.: Correcting the Cenozoic $\delta^{18}\text{O}$ deep-sea temperature record for Antarctic ice volume, *Palaeogeography, Palaeoclimatology, Palaeoecology*, 208, 195–205, 2004.
- PALAEOSSENS Project Members: Making sense of palaeoclimate sensitivity, *Nature*, 491, 683–691, 2012.
- Ritz, S. P., Stocker, T. F., and Joos, F.: A coupled dynamical ocean-energy balance atmosphere model for paleoclimate studies, *Journal of*
10 *Climate*, 24, 349–375, 2011.
- Rohling, E. J., Foster, G. L., Grant, K. M., Marino, G., Roberts, A. P., Tamisiea, M. E., and Williams, F.: Sea-level and deep-sea-temperature variability over the past 5.3 million years, *Nature*, 508, 477–482, 2014.
- Russell, G. L., Miller, J. R., and Rind, D.: A coupled atmosphere-ocean model for transient climate change studies, *Atmosphere-ocean*, 33, 683–730, 1995.
- 15 Sostdian, S. and Rosenthal, Y.: Deep-sea temperature and ice volume changes across the Pliocene-Pleistocene climate transitions, *Science*, 325, 306–310, 2009.
- Stap, L. B., Van de Wal, R. S. W., De Boer, B., Bintanja, R., and Lourens, L. J.: Interaction of ice sheets and climate during the past 800 000 years, *Climate of the Past*, 10, 2135–2152, 2014.
- Stap, L. B., De Boer, B., Ziegler, M., Bintanja, R., Lourens, L. J., and Van de Wal, R. S. W.: CO_2 over the past 5 million years: Continuous
20 simulation and new $\delta^{11}\text{B}$ -based proxy data, *Earth and Planetary Science Letters*, 439, 1–10, 2016a.
- Stap, L. B., Van de Wal, R. S. W., De Boer, B., Bintanja, R., and Lourens, L. J.: The MMCO-EOT conundrum: same benthic $\delta^{18}\text{O}$, different CO_2 , *Paleoceanography*, 31, doi:10.1002/2016PA002958., 2016b.
- Tigheelaar, M., Von Der Heydt, A. S., and Dijkstra, H. A.: A new mechanism for the two-step $\delta^{18}\text{O}$ signal at the Eocene-Oligocene boundary, *Climate of the Past*, 7, 235–247, 2011.
- 25 Van de Wal, R. S. W., de Boer, B., Lourens, L. J., Köhler, P., and Bintanja, R.: Reconstruction of a continuous high-resolution CO_2 record over the past 20 million years, *Climate of the Past*, 7, 1459–1469, doi:10.5194/cp-7-1459-2011, 2011.
- Willeit, M., Ganopolski, A., Calov, R., Robinson, A., and Maslin, M.: The role of CO_2 decline for the onset of Northern Hemisphere glaciation, *Quaternary Science Reviews*, 119, 22–34, 2015.
- Wilson, D. S., Jamieson, S. S. R., Barrett, P. J., Leitchkov, G., Gohl, K., and Larter, R. D.: Antarctic topography at the Eocene-Oligocene
30 boundary, *Palaeogeography, Palaeoclimatology, Palaeoecology*, 335, 24–34, 2012.
- Wilson, D. S., Pollard, D., DeConto, R. M., Jamieson, S. S. R., and Luyendyk, B. P.: Initiation of the West Antarctic Ice Sheet and estimates of total Antarctic ice volume in the earliest Oligocene, *Geophysical Research Letters*, 40, 4305–4309, 2013.
- Yoshimori, M., Hargreaves, J. C., Annan, J. D., Yokohata, T., and Abe-Ouchi, A.: Dependency of feedbacks on forcing and climate state in physics parameter ensembles, *Journal of Climate*, 24, 6440–6455, 2011.
- 35 Zachos, J. C., Dickens, G. R., and Zeebe, R. E.: An early Cenozoic perspective on greenhouse warming and carbon-cycle dynamics, *Nature*, 451, 279–283, 2008.

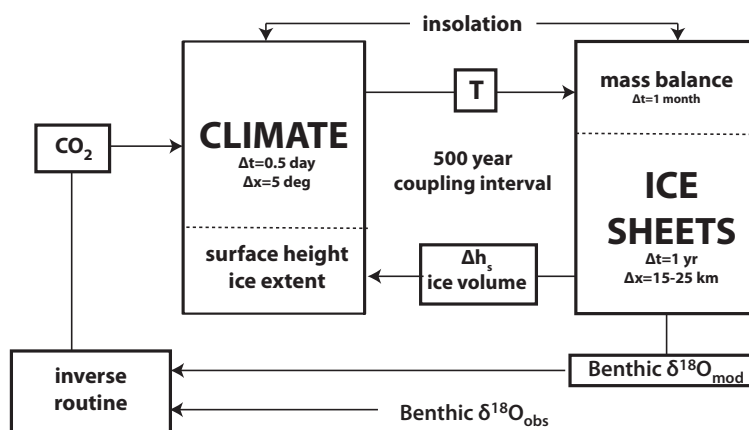


Figure 1. Schematic overview of the coupling of the zonally averaged energy balance climate model and the one-dimensional ice sheet model.

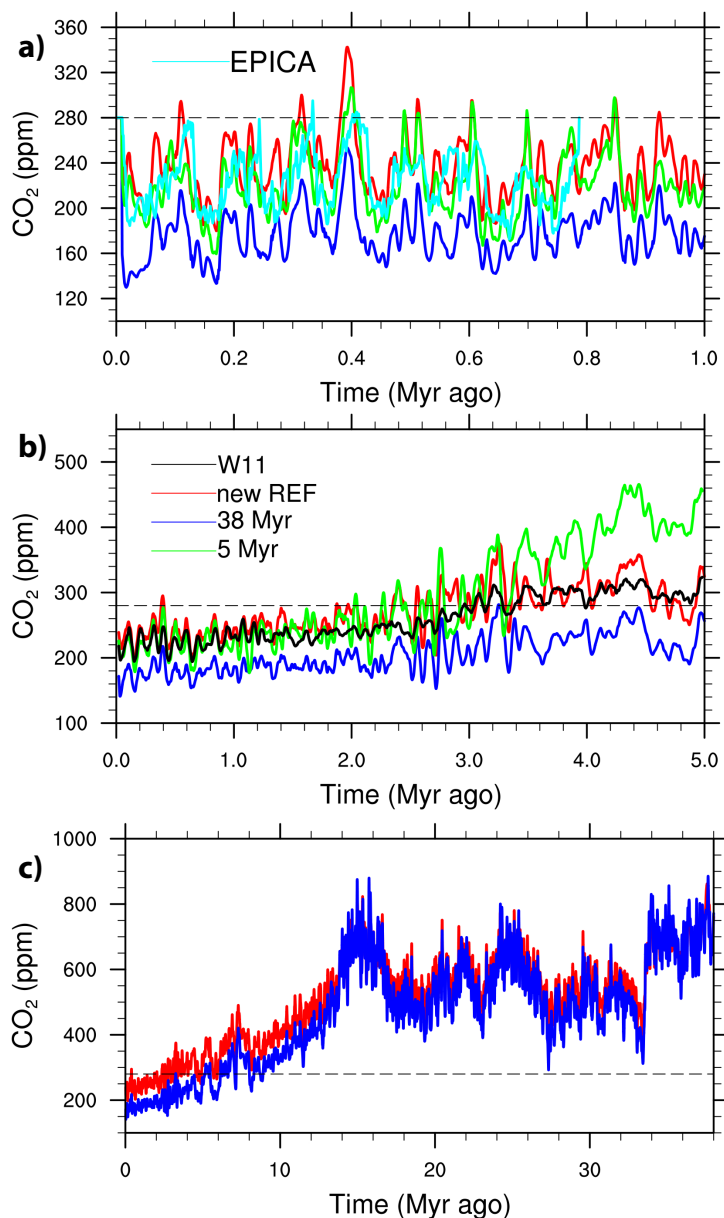


Figure 2. Atmospheric CO₂ over the past 1 Myr (a), the past 5 Myr (b) and the past 38 Myr (c). Shown are the 5-Myr run from Stap et al. (2016a) (green), the extended 38-Myr run from Stap et al. (2016b) (blue), the new reference run with altered cloud optical thickness (red), the hybrid proxy data-model reconstruction by Van de Wal et al. (2011) (W11; black) and the EPICA Dome C ice-core record (EPICA community members, 2004) (cyan). Mind the differing y-scales. The dashed line shows the pre-industrial value (280 ppm). In panel (a) we do not show 40-kyr averages, but the 1-kyr output of the model.

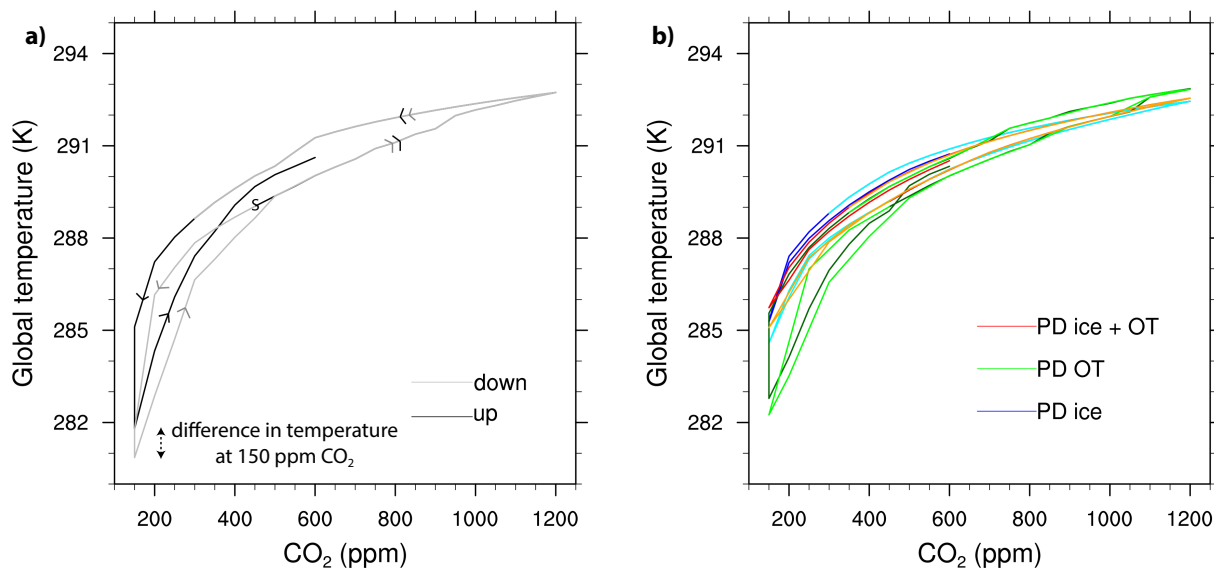


Figure 3. Relation between CO₂ and global temperature in the equilibrium runs. In (a), the fully coupled model output is shown. The startpoint of the simulation at 450 ppm CO₂ is marked by an S, and the consequent evolution for both runs is marked by colored arrows. The black line shows the up run, where CO₂ is increased first, the grey line shows the down run, where CO₂ is decreased first. At high CO₂ levels, the black line is overlaid by the grey line. In (b) the output with uncoupled ice (blue/cyan), uncoupled ocean overturning strength (darkgreen/green) and both these factors uncoupled (red/orange) are shown. The darker colors (blue, darkgreen, red) show the up runs, the lighter colors (cyan, green, orange) show the down runs. The startpoint and evolution are the same as in (a).

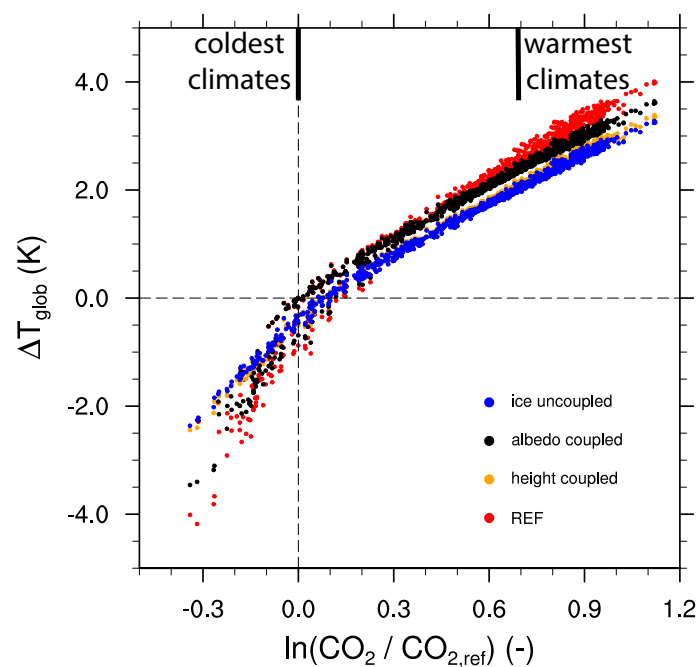


Figure 4. Relation between the logarithm of CO₂ divided by the PI value of 280 ppm, and global temperature anomalies with respect to PI (of the reference run), for the reference simulation (red dots), the simulation with uncoupled ice (blue dots) and the simulation with only surface height (orange dots) or albedo (black dots) coupled.

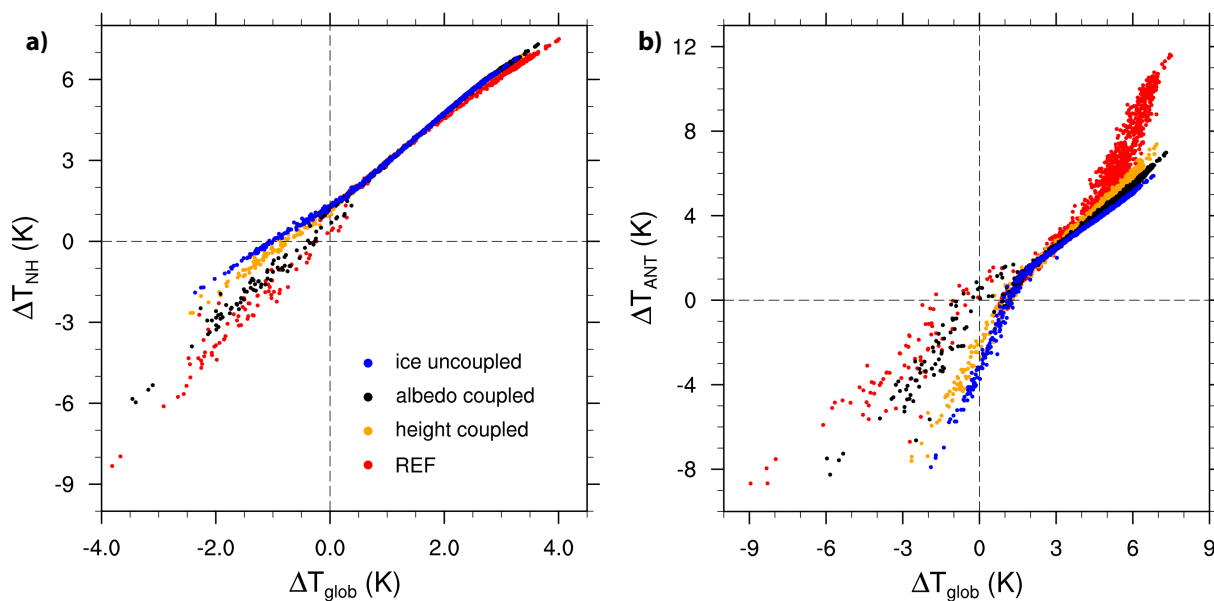


Figure 5. Relation between anomalies with respect to PI (of the reference run) of global temperature, and (a) Northern Hemispheric temperature (40 to 80° N), and (b) Antarctic temperature (60 to 90° S), for the reference simulation (red dots), the simulation with uncoupled ice (blue dots) and the simulation with only surface height (orange dots) or albedo (black dots) coupled.

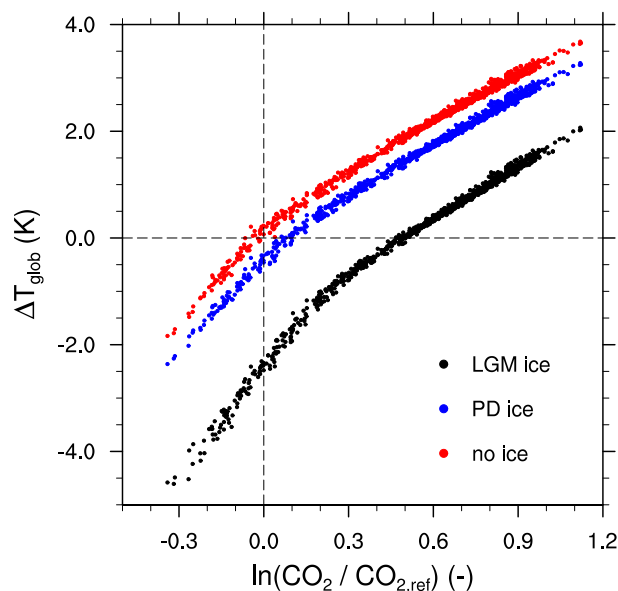


Figure 6. Relation between the logarithm of CO₂ divided by the PI value of 280 ppm, and global temperature anomalies with respect to PI (of the reference run), for the simulation with ice kept at PD level (blue dots), at LGM level (black dots) and the simulation with all land ice removed (red dots).